Electronic Supplementary Material (ESI) for Nanoscale.

Supplementary Information

Spin Wave Driven Skyrmion based Diode on T-shaped Nanotrack

Shipra Saini[a], Namita Bindal[a], Ravish Kumar Raj[a], and Brajesh Kumar Kaushik [a]

[a]*Department of Electronics and Communication Engineering,*

Indian Institute of Technology Roorkee, Roorkee, Uttarakhand, India-247667

A. Effect of Dzyaloshinskii–Moriya interaction (DMI) on the edges of nanotrack

Recent observation of chiral magnetic textures in thin films has highlighted the crucial role of the Dzyaloshinskii-Moriya interaction (DMI) in dictating the chirality of magnetization rotations. The most remarkable consequence of DMI is the emergence of topologically protected magnetization configurations called skyrmions. In nanotrack, DMI leads to a specific form of micromagnetic boundary conditions. Close to the sample edges, the presence of DMI gives rise to a twist in the magnetization away from the z axis as shown in Fig. S1. The z component of the magnetization for the 100-nm-width sample is in uniform state at and near x=0 nm. A canting away from the z direction is visible near the edges of the nanotrack. A skyrmion initially positioned at the nucleation point on the nanotrack gets drifted by spin wave driving force. Indeed, when the skyrmion approaches the edge, the ferromagnetic background landscape changes because of the nonuniformity induced at these edges due to DM interaction [1]. This interaction between the skyrmion and the edge induces a force (F_{edge}) exerted by the surface and this force can be described by an exponential function of the skyrmion-edge distance as follows [2]:

$$F_{edge} = - V_{edge} \nabla \left[exp\left(- \frac{\left(y - \frac{w}{2} \right)}{L_{edge}} \right) + exp\left(\frac{\left(y + \frac{w}{2} \right)}{L_{edge}} \right) \right]$$

Here, V_{edge} is the potential strength of this repulsive force and L_{edge} is the penetration depth of the magnetization twist being induced by the DMI at the edges of the nanotrack. As it reaches towards the edges of the nanotrack, it gets repelled by the edge twist of the magnetization [2, 3].

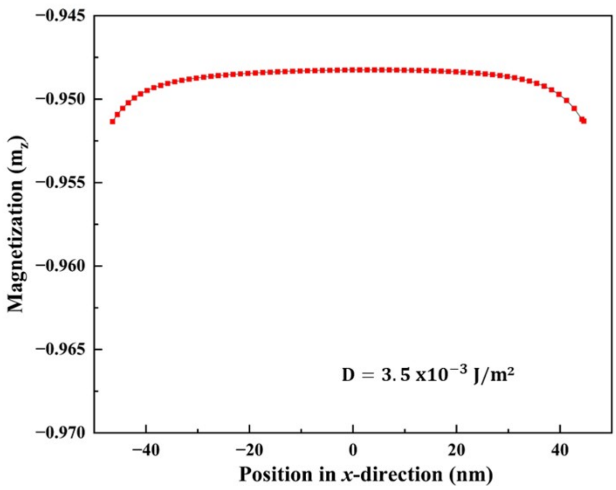

Figure S1. Magnetization rotation at the edges of the nanotrack with interface DMI. Magnetization profile on a nanotrack of 100 nm long and 100 nm wide with initial magnetization along the z direction and for D = 3.5 mJ/m^2.

B. Forces acting on the spin wave driven skyrmion

The dynamics of spin wave driven skyrmion is mainly influenced by the forces due to scattering, edge repulsion, and spin wave as shown in Fig. S2. When the spin wave impinges the skyrmion, the skyrmion moves either away from source or far from source. The forces responsible for this motion induces due to the scattering of spin wave on skyrmion. The scattering force ($\vec{F}_{sc}$) acting on the skyrmion is given as follows [4]:

$$\vec{F}_{sc} = \vec{F}_{\parallel} + \vec{F}_{\perp} = J_{sw} e^{-\frac{r.\vec{x}}{l_{sw}}} k[\sigma_{\parallel}\vec{x} + \sigma_{\perp}\vec{y}]$$

where, J_{sw} and k are the spin wave current density and wave vector. The parameter $l_{sw} = (\alpha^{-1}(m\pi f/\hbar)^{-1/2})$ is responsible for spin wave decay as a function of Gilbert damping. respectively. The force is the function of the scattering cross section (σ) of the skyrmion. The energy dependent longitudinal ($\sigma_{\parallel}$) and transversal ($\sigma_{\perp}$) scattering cross section can be expressed as follows [5]:

$$\begin{pmatrix} \sigma_{\parallel} \\ \sigma_{\perp} \end{pmatrix} = \int_0^{2\pi} \begin{pmatrix} 1 - cos\theta \\ -sin\theta \end{pmatrix} \frac{d\sigma}{d\theta} d\theta$$

Here, θ is the scattering angle of spin wave and skyrmion. On solving the Thiele equation of skyrmion motion with this scattering force, the skyrmion velocity comes as a function of $\begin{pmatrix} -\sigma_{\perp} \\ \sigma_{\parallel} \end{pmatrix}$ [5]. For high energy magnon, transversal cross section dominates and drives the skyrmion towards the spin wave source. Whenever skyrmion reaches close to the edges of the nanotrack, there will be an interaction between skyrmion and edges of the nanotrack. This interaction between the skyrmion and the edge induces a force (F_{edge}) exerted by the surface and this force can be described by an exponential function of the skyrmion-edge distance as follows:

$$F_{edge} = -V_{edge}\nabla\left[exp\left(-\frac{\left(y - \frac{w}{2}\right)}{L_{edge}}\right) + exp\left(\frac{\left(y + \frac{w}{2}\right)}{L_{edge}}\right)\right]$$

Here, V_{edge} is the potential strength of this repulsive force and L_{edge} and w are the penetration depth of the magnetization twist being induced by the DMI at the edges of the nanotrack and width of the nanotrack, respectively. The F_{edge} balances the transversal scattering force and results the motion of the skyrmion in spin wave direction. Hence, the width of the nanotrack plays the crucial role to achieve the proposed diode functionality with spin wave driven skyrmion. In this work, the width of the nanotrack is chosen to suppress the motion of skyrmion towards spin wave source.

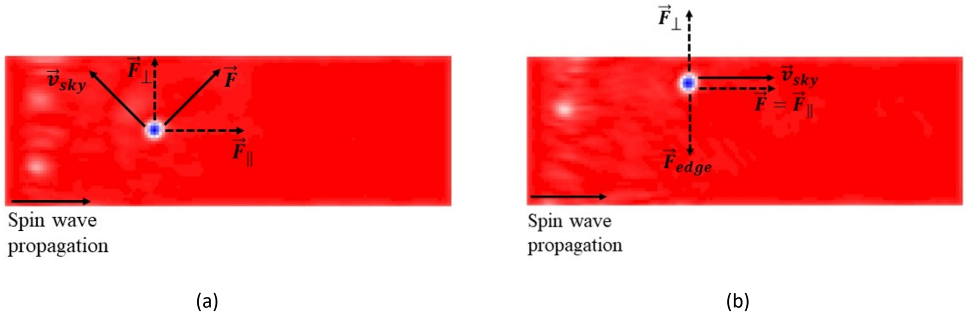

(a) (b)

Figure S2 (a) Spin wave driving force on a skyrmion far away from the edges of the nanotrack and (b) spin wave force when the skyrmion is near enough to the edge to experience the edge repulsion force.

C. Interaction of spin wave with skyrmion

To further investigate the interaction between the spin wave and skyrmion, the motion of the spin-wave driven skyrmion on a 400 nm long and 60 nm wide nanotrack is studied, without considering the mid-arm region. Fig. S3(a) shows the variation

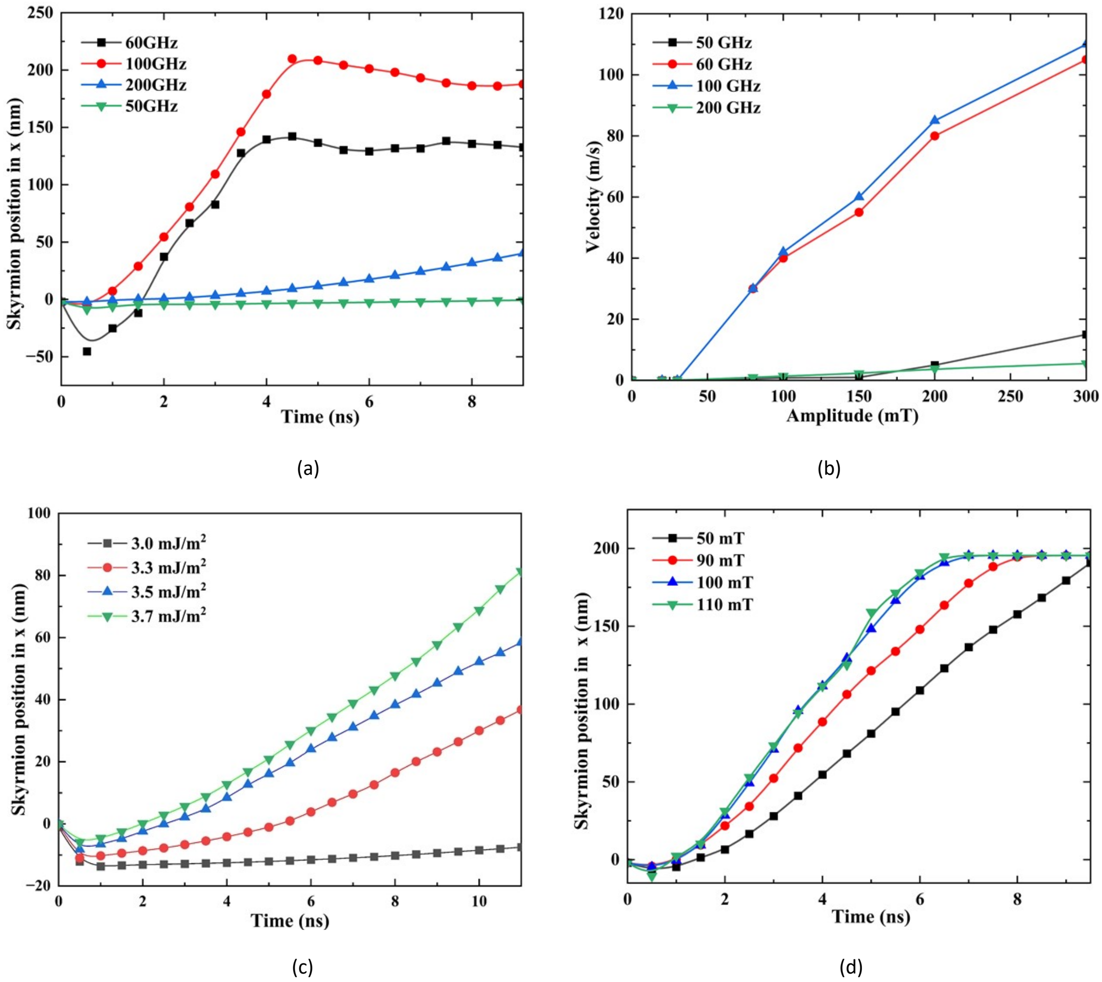

Figure S3 (a) Skyrmion position as a function of the spin wave frequencies with $H_0 = 0.2\ T$, (b) Velocity of skyrmion as a function of field amplitude with different frequencies, (c) Skyrmion position with different DMI with $f = 50\ GHz$ and $H_0 = 0.2\ T$, and (d) Skyrmion position as a function of the spin wave amplitude with $f = 60\ GHz$

of skyrmion position with respect to time for different frequencies of RF field. Here, the amplitude of the excitation field is considered as $0.2\ T$. When the spin wave impinges on the skyrmion, they either get reflected or scattered through the skyrmion. Moreover, when spin wave frequency is greater than a threshold value ($f = 50\ GHz$), the skyrmions can be drifted in the direction of the SWs propagation. For $f < 50\ GHz$, the skyrmion does not move at all and pinned near the nucleation point. This is due to the fact that when the wavelength of spin wave is large as compared to the skyrmion size, only a smaller surface of the skyrmion interacts with the spin wave [6]. Hence, there will be negligible transfer of momentum resulting in negligible driving force from the spin wave. For $f = 60\ GHz$, initially the spin wave is partially transmitted through the skyrmion leading to transfer of momentum from the spin wave to the skyrmion that exerts a spin torque on the skyrmion in accordance with the conservation of momentum. As a result, initially, the skyrmion propagates slightly in the direction opposite to the propagation of spin wave. However, after sometime, it is observed that spin wave completely gets reflected from the skyrmion and push it away from the source in $+x$ direction. It is also noted that at $f \geq 200\ GHz$, the spin wave propagates across the skyrmion without being scattered, hence no driving force acts on the skyrmion. However, to display the relationship of RF field amplitude and frequency with the dynamics of skyrmion, the velocity of skyrmion with respect to the amplitude of RF field ranging from $0 - 0.3\ T$ is plotted (Fig. S3(b)) for different frequencies. However, if the size of the skyrmion is increased by increasing the DMI value, then surface interaction of the skyrmion with spin wave increases that results in change in position of the skyrmion even at $f = 50\ GHz$ as shown in Fig. S3(c). Alternatively, this can be done by decreasing the magnetic anisotropy [7]. This is because the size of the skyrmion decreases with increase in anisotropy [7]. In order to obtain more quantitative information of the dependence of the skyrmion position on RF field amplitude, the position of skyrmion with respect to time at different RF field amplitudes for $f = 60\ GHz$ is illustrated in Fig. S3(d). It is observed that the skyrmion takes less time to reach toward the end of the nanotrack with increasing amplitude of the RF field. This is due to the fact that large field amplitude transfers more magnetic momentum to the skyrmion. Moreover, with the large width of the nanotrack, the skyrmion does not move forward instantly in absence of the sufficient repulsive forces from the far away boundaries. Once, the skyrmion reaches to the boundaries, then it starts to move forward in the direction of spin wave propagation. It is observed that in order to achieve the one-way functionality at high speed, the main objective is to move the skyrmion instantly with the impinging of spin waves that is obtained when the nanotrack width is considered as 60 nm. Hence, it can be said that the dimension of the nanotrack plays a crucial role in achieving the diode functionality. Furthermore, Fig. S4 shows the plot for applied RF magnetic field and corresponding m_x and m_z component for spin wave propagation.

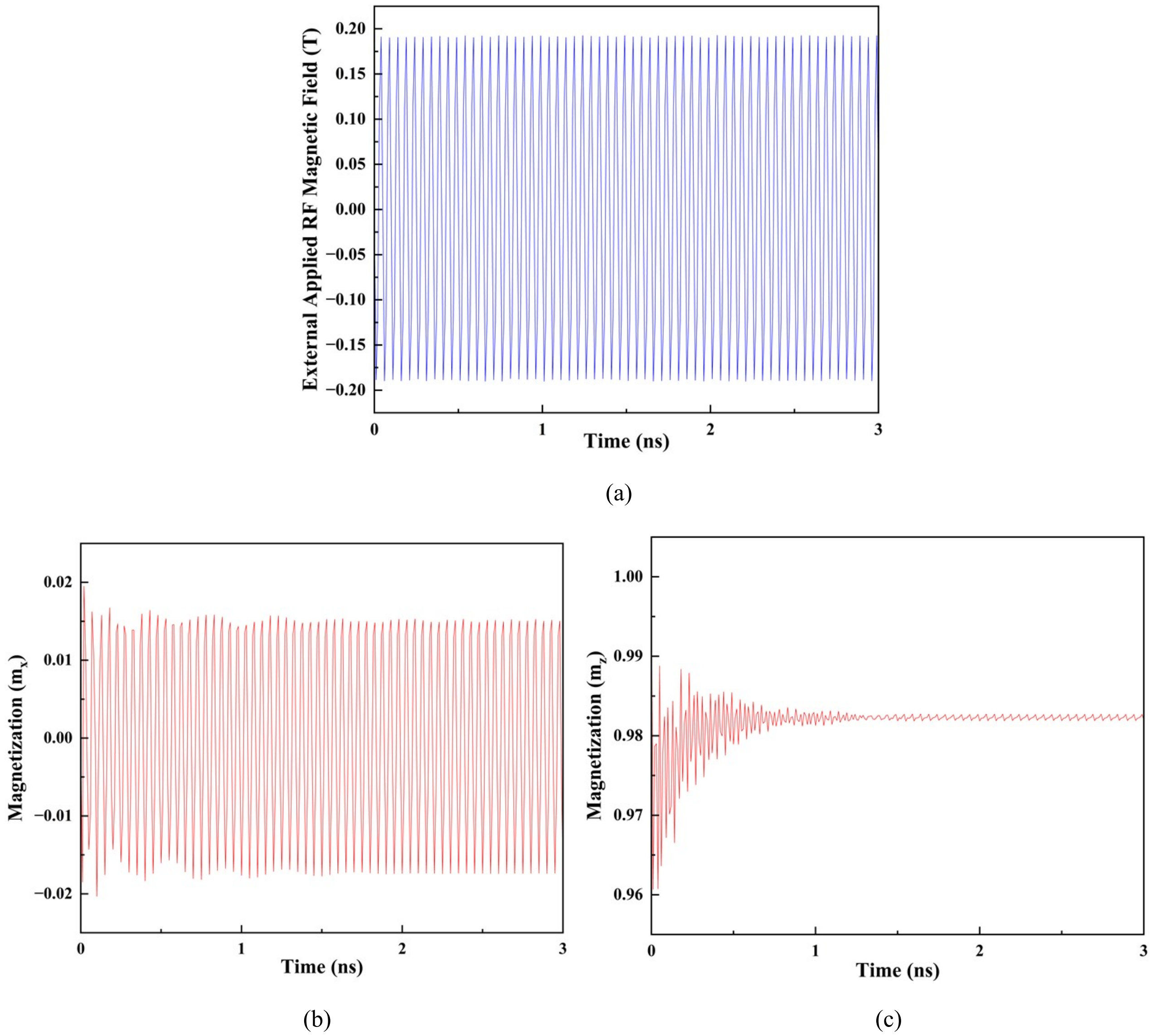

Figure S4 (a) Externally applied sinusoidal magnetic field for spin wave generation, (b and c) magnetization component in x and z direction, respectively.

D. Diode functionality with multiple skyrmions

Analysis with multiple skyrmions in forward and reverse motion has been performed on T-shaped nanotrack. During the motion from left to right, all the skyrmions travels to detection region without deviating even in less time. This is due to the fact that there is skyrmion-skyrmion interaction among them. Moreover, from right to left motion, most of the skyrmions gets annihilated at the mid arm corner. However, due to force generated by skyrmions interactions, one skyrmions gets push into the mid arm region and stuck over there as shown in Fig. S5. It is observed that diode functionality can be achieved with an array of skyrmions on this T-shaped nanotrack.

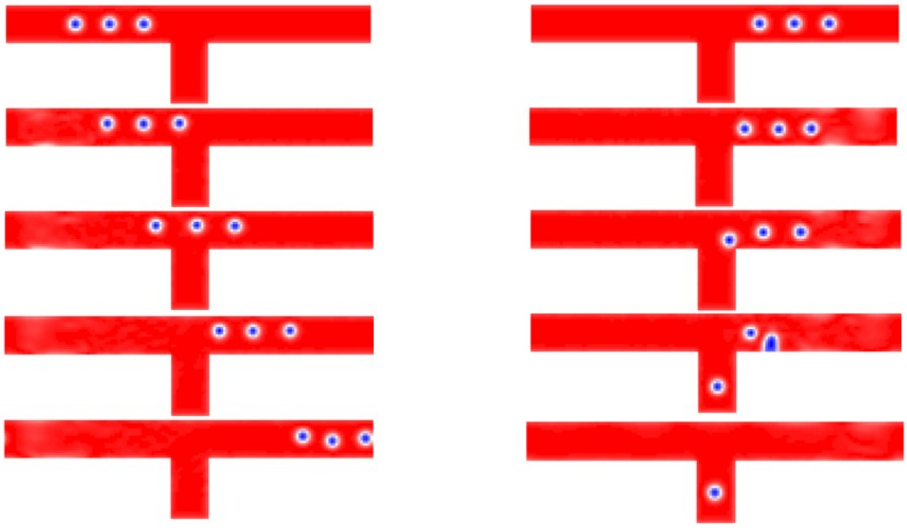

(a) (b)

Figure S5. Micromagnetic snapshots with multiple skyrmions (a) forward motion and (b) reverse motion.

E. Effect of the edge roughness on the proposed device

To make our device realistic, we have now incorporated edge roughness in the device. It is observed that the device is working properly for forward and reverse moving skyrmion as shown in Fig. S6.

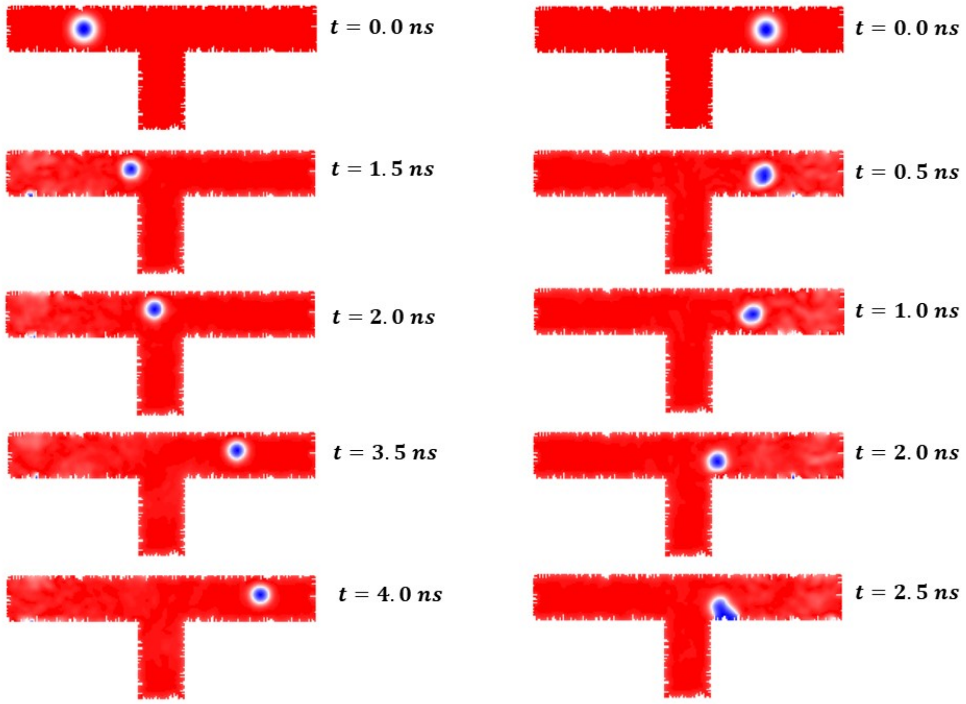

(a) (b)

Figure S6 Micromagnetic snapshots for (a) forward moving skyrmion and (b) reverse moving skyrmion in the presence of edge roughness on the nanotrack.

References:

1. C. Navau, N. Del-Valle, and A. Sanchez, *Physical Review B*, 2016, 94, 184104.
2. X. Zhang, J. Muller, J. Xia, M. Garst, X. Liu, and Y. Zhou, 2017, 19, 065001.
3. S. Rohart and A. Thiaville, *Physical Review B*, 2013, 88, 184422.
4. C. Schütte and M. Garst, *Physical Review B*, 2014, 90, 094423.
5. X. Liang, J. Xia, X. Zhang, M. Ezawa, O. A. Tretiakov, X. Liu, L. Qiu, G. Zhao, and Y. Zhou, *Applied Physics Letters*, 2021, 119, 062403.
6. X. Zhang, M. Ezawa, D. Xiao, G. P. Zhao, Y. Liu, and Y. Zhou, *Nanotechnology*, 2015, 26, 225701.
7. W. Jiang, G. Chen, K. Liu, J. Zang, S. G. Te Velthuis, and A. Hoffmann, *Physics Reports*, 2017, 704, 1-49, 2017.